SET 2023

NOTTINGHAM

20th International Conference on Sustainable Energy Technologies

15th to 17th August 2023, Nottingham, UK

Sustainable Energy Technologies 2023

Conference Proceedings: Volume 1

Proceedings of the
20th International Conference on
Sustainable Energy Technologies
SET 2023
15th – 17th August 2023, Nottingham, UK

Edited by
Professor Saffa Riffat

SET 2023 Admin Support
Department of Architecture and the Built Environment
Faculty of Engineering, University of Nottingham

Supported by the Conference Organising Committee:

Chair: Professor Saffa Riffat
Professor Yuehong Su
Dr Emmanuel Tapia-Brito
Dr Ziwei Chen

Reference to a conference paper:

To cite a paper published in these conference proceedings, please substitute the highlighted sections of the reference below with the details of the article you are referring to:

Author(s) Surname, Author(s) Initial(s), 2023. 'Title of paper'. In: Riffat, Su,. ed., **Sustainable Energy Technologies**: Proceedings of the 20th International Conference on Sustainable Energy Technologies, 15th – 17th August 2023, Nottingham, UK. University of Nottingham: Buildings, Energy & Environment Research Group. Pp XX-XX. Available from: nottingham-repository.worktribe.com/ [Last access date].

ISBN-13: 978 085358 357 8

Version: 15.12.2023

Foreword

SET2023 in Nottingham, UK, continued the tradition of this esteemed annual conference, building upon the momentum regained in 2022 after a 2-year hiatus due to COVID-19.

The 20th International Conference on Sustainable Energy Technologies was a pivotal international academic conference in the realm of global sustainable energy. The conference served as a platform for the exchange of the most recent technical insights, the dissemination of current research findings, and the discussion of major challenges that could influence the future trajectories of human society, such as sustainable energy technology research, its applications, and energy security.

Held from August 15th to 17th, 2023, in Nottingham, UK, the conference was a collaborative effort between the World Society of Sustainable Energy Technologies (WSSET) and the University of Nottingham. Distinguished experts and scholars in the field, as well as representatives from eminent enterprises and universities, convened to deliberate on new advancements and accomplishments in the sector, whilst fostering academic exchange, the practical application of scientific discoveries, and collaborations between universities and industries, as well as between governments and industries.

The papers included in these proceedings concentrated on the same key topics as the previous year, such as Energy Storage for the Age of Renewables; Research, Innovation and Commercialisation in Sustainable Energy Technologies; Integrating Planning & Policy, Architecture, Engineering & Economics; Energy and Environment; Engineering Thermo-physics; and Systemic Change for Cities.

Over 200 delegates attended SET2023, with nearly 350 abstracts received. Although the number of papers presented and posters displayed is yet to be confirmed, the conference was a rich forum for academic and practical discourse.

We extend our gratitude to all participating authors for their invaluable contributions to both the conference and the publishing of this book. Our international scientific committee deserves special mention for their advisory role and their meticulous review of papers. We also express our unreserved thanks to Zeny Amante-Roberts and Celia Berry for their relentless efforts in making SET2023 a successful event. A special acknowledgement goes to our sponsors PCM Products Ltd., Terry Payne, and the newly added Stormsaver Ltd, for their generous support.

Professor Saffa Riffat
Chair in Sustainable Energy Technologies
President of the World Society of Sustainable Energy Technologies
SET 2023 Chair

CONTENTS

Paper Reference # | **Title of Paper** | **Page Number**

#48: Rapid evaluation of buildings thermal performance using infrared thermography and artificial intelligence

Arijit SEN[1], Amin AL-HABAIBEH[2]

[1] Research Fellow, Product Innovation Centre, Nottingham Trent University, Email: arijit.sen@ntu.ac.uk
[2] Director of Product Innovation Centre, Nottingham Trent University, Email: amin.al-habaibeh@ntu.ac.uk

Abstract: Domestic energy consumption significantly contributes to the UK's overall energy usage. Space and water heating are responsible for most households' energy consumption. Any price hike, such as the current energy price situation, would seriously affect the budget of many households living in poorly insulated buildings. Improving insulation by deep retrofitting of existing buildings is expected to be a reasonable solution for reducing the domestic heating energy demands for those households. However, the level of insulation is a key issue, as retrofitting with excess insulation will incur higher cost and result in longer payback periods, especially in countries with moderate temperatures such as the UK. Therefore, it is necessary to estimate the thermal performance of existing building stock at the planning stage of retrofitting. Such evaluation of thermal performance requires, in most cases, prolonged monitoring of buildings using sensors installed for data analysis leading to significant time and cost issues. To address this knowledge gap and provide rapid evaluation of expected energy savings of retrofitting, this paper presents a novel technology with a case study to estimate energy savings between insulated and uninsulated residential buildings using Infrared Thermography and Artificial Intelligence. The results prove that the suggested AI technology, combined with infrared thermography, can provide rapid evaluation of heat losses through the building envelop and estimate the potential energy savings due to the enhancement of wall insulation by retrofitting.

Keywords: Retrofitting; Infrared thermography; Artificial Intelligence; Neural Networks; Insulation; Insulation.

1. INTRODUCTION

The increase in market economy activities, particularly during the post-COVID era, has resulted in a surge in energy demand in 2021, which is still growing but at a slower rate (Ritchie, Roser and Rosado, 2022). The recent global situation has affected household energy prices, increasing them globally by 112.9% (Guan *et al.*, 2023). Despite the growth of renewable energy, fossil fuels still dominate energy production (BP PLC, 2021). Buildings contribute significantly to greenhouse gas emissions (UN Environment Programme, 2020), with heating responsible for around 80% of domestic energy consumption in the UK (Department for Business Energy & Industrial Strategy, 2023). Although a case study has proven that newly built houses in England and Wales have lower energy demand (The National Energy Efficiency Network, 2019), a significant number of English dwellings fall into the category of poor energy efficiency in existing housing stock, with 75% of houses being pre-1990 constructions (Piddington *et al.*, 2020). The UK Government is considering strategies to reduce energy consumption in buildings, such as improving insulation and energy efficiency, to meet their goal of net-zero emissions by 2050 (Government Property Agency, 2022).

Wall insulation plays a crucial role in improving energy efficiency, but its effectiveness depends on various factors, such as local weather, insulation materials, level of insulation (U-value), and occupants' behaviour, including working from home (Al-Habaibeh et al., 2021) or opening of windows (Salim and Al-Habaibeh, 2023). A wide variety of insulation materials are commercially available in today's market, which are classified as organic materials, inorganic materials, combined materials, and new technology materials (Papadopoulos, 2005;Sadineni, Madala and Boehm, 2011). Understanding how these different types of insulation materials impact energy savings is important. Tabrizi, Hill and Aitchison, (2017) conducted a study to investigate the impact of different insulation materials and thicknesses on energy consumption in a multi-story residential building in Sydney. The authors tested six types of insulation materials at three different thicknesses (30mm, 60mm, and 90mm). The study found a significant range variation in heating energy consumption. The most effective insulation material for saving heating energy was extruded polystyrene. Therefore, selecting the right insulation material is crucial for optimizing energy savings, as well as considering other factors such as environmental impact, resistance to sound, moisture, and fire. However, cost of materials and installation will need to be taken into consideration. Insulation can be applied to both internal and external surfaces of a building's wall, known as internal and external insulation, respectively. Theoretically, the effectiveness of insulation depends on its layer's thickness rather than its placement. However, in reality, the thermal performance of walls after retrofitting with improved insulation varies based on whether they are internally or externally insulated and the building's location and climate (Kossecka and Kosny, 2002). Several studies have explored the energy performance of externally and internally insulated walls and the changes in energy performance due to retrofitting in different climates. Some studies found external wall insulation to be more effective (Kim and Moon, 2009;Kolaitis *et al.*, 2013), while others favoured internal wall insulation (Reilly and Kinnane, 2017;Wang *et al.*, 2016). Internally insulated buildings consume less energy but have reduced available indoor space, leading to a trade-off between space requirements and energy demand reduction (Reilly and Kinnane, 2017). On the other hand, buildings with external insulation have better thermal stability (Wang *et al.*, 2016); but the appearance, for example, of heritage buildings in such situations will not be preserved.

Infrared thermography is a quick and effective way of evaluating the post-retrofit effectiveness of wall insulation. Infrared radiation from objects make infrared thermography, following suitable calibrations, a useful tool for non-contact measurement of walls surface temperature (Marino, Muñoz and Thomas, 2017). It is also useful for estimating the thermal transmittance in a non-invasive way, such as through a building's windows (Baldinelli and Bianchi, 2014), heat loss through door openings (Al-Habaibeh, Medjdoub and Pidduck, 2012), and characterizing the thermal performance of building facade (Bienvenido-Huertas *et al.*, 2019). Several researchers have demonstrated the successful use of this technology, for example, the estimation of heat flow rate through a thermal bridge (O'Grady, Lechowska and Harte, 2017), estimation of time shift values of temperature in building elements, and investigation of transient temperature response behaviour over time (Xie *et al.*, 2019). Moreover, infrared thermography can be used to calculate thermal power and heat losses through a building's walls (Albatici and Tonelli, 2010; Albatici, Tonelli and Chiogna, 2015; Nardi, Sfarra and Ambrosini, 2014).

Artificial intelligence has been significantly used in many research studies to predict energy consumption in buildings. Among them, Artificial Neural Networks (ANNs) have been most widely used due to their suitability over conventional statistical methods (Wang and Srinivasan, 2017; Deb *et al.*, 2017). These studies have tested various types of ANNs, including feedforward and recurrent neural networks, and have used different input variables. The feedforward neural network is suitable for regression, classification, and pattern recognition tasks (Gori, 2018). On the other hand, recurrent neural networks can be successfully applied to time series problems. However, they have a limitation in terms of vanishing gradients (Haykin, 2000). To overcome this limitation, Hochreiter and Schmidhuber (1997) developed a special type of recurrent neural network called Long Short-Term Memory (LSTM) network. The LSTM network is equipped with memory blocks that process information through different gates, such as forget gate, peephole, input gate, and output gate. These gates allow the memory blocks to selectively remember or forget information, allowing the LSTM network to overcome the vanishing gradient problem (Witten *et al.*, 2017). ANNs can achieve high accuracy in predicting energy consumption and can outperform other methods, such as energy simulation software (Naji *et al.*, 2016; Martellotta *et al.*, 2017; Wang, Lee and Yuen, 2018). Retrofitting with enhanced insulation can improve the energy efficiency of existing buildings (Al-Habaibeh *et al.*, 2022), but estimating energy savings prior to retrofit and the payback period of investments is a challenging task.

Previous research shows that by combining infrared thermography and ANN, it is possible to predict future heat losses through buildings' walls from midterm (around 8 years) historical climate data with reasonable accuracy (Al-Habaibeh, Sen, and Chilton, 2021). However, the study does not estimate energy savings. In the current paper, we use infrared thermography and ANN to estimate energy savings due to retrofitting.

2. METHODOLOGY

The steps involved in the heat loss prediction and energy savings estimations by combining infrared thermography and ANN is presented in Figure 1. To calculate the heat loss per square meter of a building's wall, we use the thermal power approach developed by Albatici and Tonelli (2010), as shown in Equation 1.

Equation 1: *Thermal power* $P = 5.67\varepsilon_{tot}\left(\left(\frac{T_s}{100}\right)^4 - \left(\frac{T_{ext}}{100}\right)^4\right) + 3.8054v(T_s - T_{ext})$

Where:

- T_{ext} = outdoor temperature
- v = wind speed
- Ts = external wall surface temperature
- ε_{tot} = emissivity

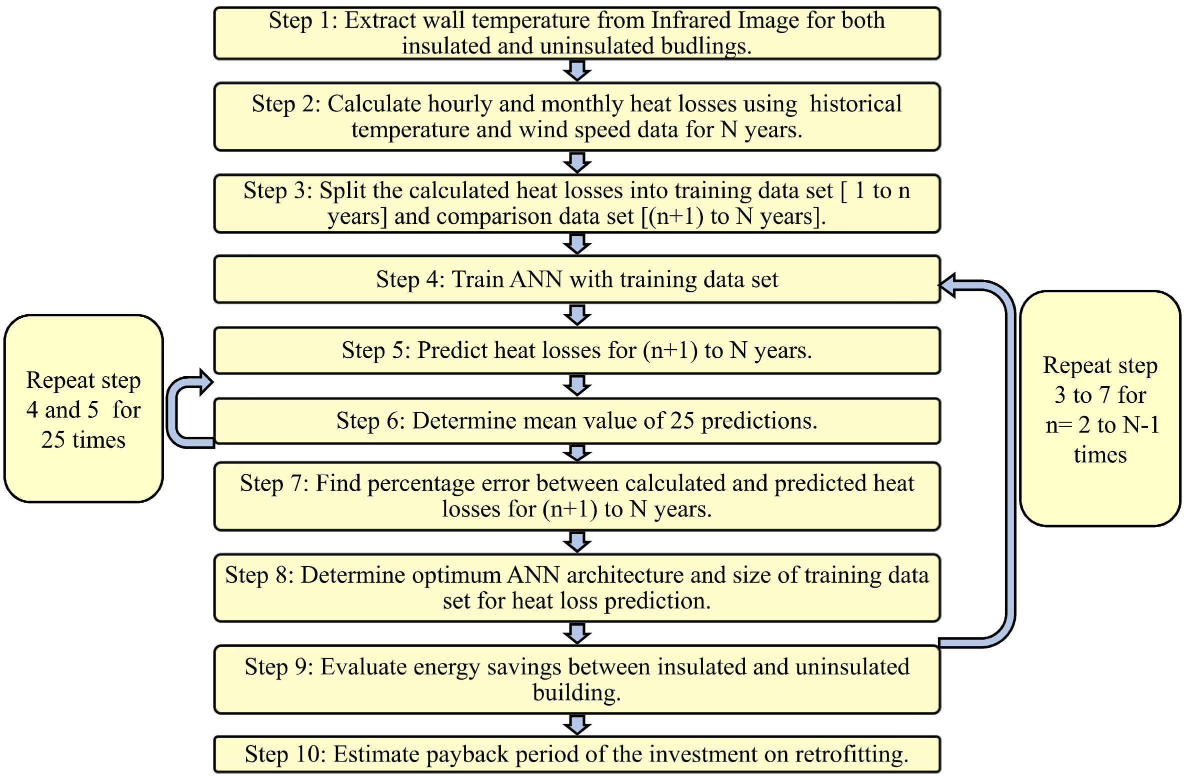

Figure 1 A schematic representation of the research methodology; adopted from Al-Habaibeh, Sen, and Chilton (2021)

By taking into account the external wall surface temperature in relation to the respective outdoor temperature at the moment when the infrared image is captured as an initial point; and 20°C as the secondary point, a linear curve can be generated. Such linear curves are used for the case study in this paper are illustrated in Figure 2. The external wall surface temperatures necessary for calculating heat loss using Equation 1; and are extracted from this linear curve at different outdoor temperatures. For plastered brick walls, the emissivity is considered to be 0.93 (CIBSE, 2006). If 1 W/m^2 of heat is radiated for one hour, it will be equivalent to 1 Wh/m^2 of heat energy transfer. Therefore, the value of P for each hour, calculated from equation 1, can be considered as the hourly heating energy loss per square meter of the building's wall. Equation 2 expresses the average heat loss in any given hour i in a given month j through per square meter of a wall, P_{ij}. The heat loss P_i is obtained using equation 1. Likewise, equation 3 expresses the total heat loss in each calendar month in a year as the summation of hourly heat losses in that month.

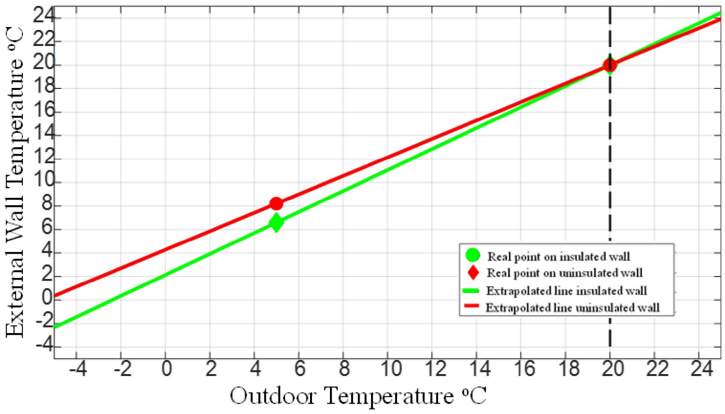

Figure 2 The assumed relationship between outdoor temperature and external wall temperature

Equation 2: Heat loss at i^th hour of each day in j^th month $P_{ij} = \frac{1}{n}\sum_{n=1}^{D} P_i$

Where:

- i= 00:00 to 23.00.
- j = January to December.
- D = the number of days in j^{th} month of a given year

Equation 3: Total heat loss through a building's wall in a calendar month $P_m = \sum_1^D \sum_1^{24} P$

Where:

- D = number of days in that month and
- P = hourly heat loss obtained using equation 1.

Using historical local weather data, the hourly average heat loss and the monthly total heat loss for N years are calculated. These values are then divided into training and test data sets for neural network analysis. Different combinations of training and test data sets are formed, ranging from 2 years to N-1 years. The training data set is used to train the neural network, and the test data set is used to evaluate its performance. Performance evaluation is conducted considering percentage errors, which are calculated using equations 4 and 5, respectively.

Equation 4: Error $e = \sum_{i=1}^{n}(Y_i - P_i)$

Where:

- Y = ANN predicted heat loss and
- P = calculated heat loss from equation 2 for hourly averaged heat loss and the same from equation 3 for monthly total heat loss, respectively.
- n = 288 (24×12) in case of hourly average heat loss and 12 in case of monthly total heat loss

Equation 5: Percentage error $e_p = \frac{|e|}{\sum_{i=1}^{n} P_i} \times 100$

Where:

- e = error calculated using equation 4.
- P = calculated heat loss from equation 2 for hourly averaged heat loss and the same from equation 3 for monthly total heat loss, respectively.
- n = 288 (24×12) in case of hourly average heat loss and 12 in case of monthly total heat loss

3. CASE STUDY

A case study was conducted in two buildings located in Nottingham, England: an externally insulated mid-terraced building and an uninsulated end-terraced building. Figure 3 displays an infrared image of the adjacent buildings taken on February

12th at around 8:30 pm using a FLIR T640 thermal camera during a thermographic survey. The ambient temperature during the survey was 5°C. The Thermacam Quick Report software from FLIR was utilized to extract the pixelwise temperature values from the infrared image of the buildings.

3.1. Analysis of infrared image

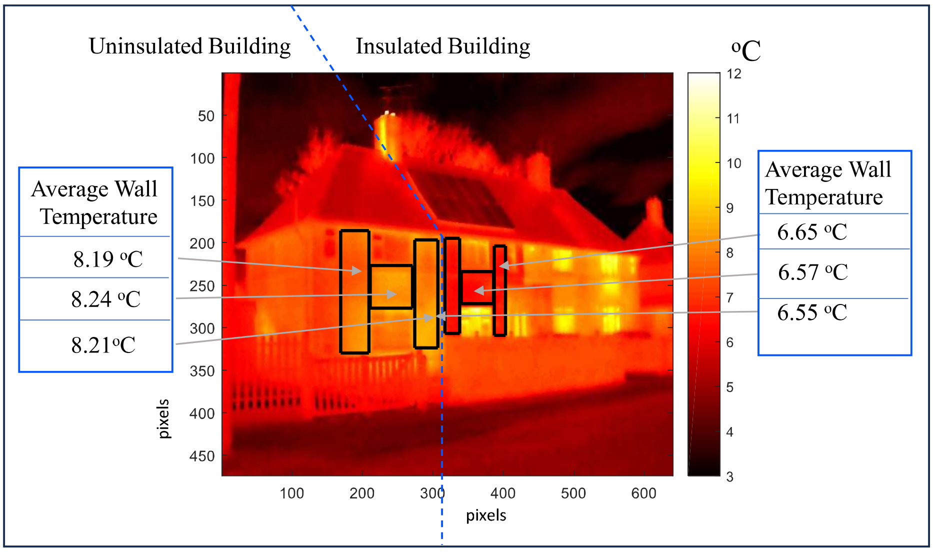

Figure 3 An infrared image of the insulated and the uninsulated house

In Figure 3, the average wall surface temperature is marked for different sections of both the insulated and uninsulated buildings. The average wall surface temperature for various sections of the uninsulated building ranges from 8.19°C to 8.24°C. In contrast, the wall surface temperature for different sections of the insulated building ranges from 6.55°C to 6.65°C. Additionally, Figure 3 shows that the insulated building has photovoltaic solar cells on its roof to enhance its energy efficiency. The temperature difference in the average wall surface temperature between the two buildings is approximately 1.6°C. Figure 4 displays the temperature profile along line ABCD in the infrared image, where the wall surface temperature values along AB represent the uninsulated building, BC represents the insulated building, and CD represents another uninsulated building adjacent to the insulated one.

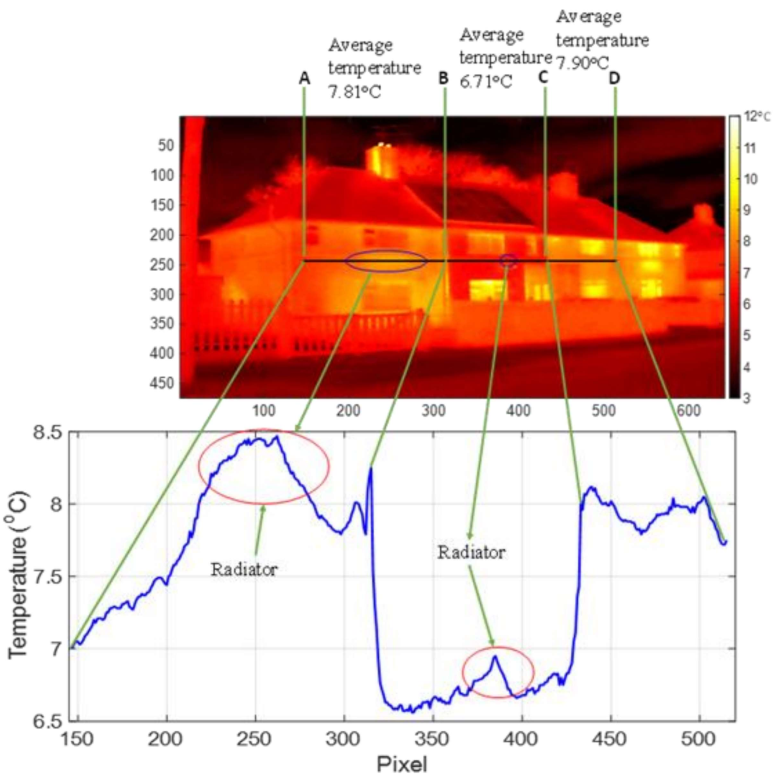

Figure 4 Temperature profiles generated from the infrared image

3.2. Heat loss calculations

Equation 1 is utilized to calculate the heat transfer through the building's wall in W/m^2 for both case studies, which is then multiplied by 1 to convert it into heat energy loss in Wh/m^2. The wall surface temperature Ts is first extracted from the infrared image and then interpolated against the external temperature to estimate the historical heat loss. The outdoor ambient temperature T_{ext} and wind speed v are obtained from weather station observations. The hourly average and monthly total heat losses are calculated by extracting the historical hourly ambient temperature and hourly wind speed between 2004 and 2019 from the Met Office database (2019) for the location of the case studies. The hourly average heat loss is determined by calculating the average heat loss for all days for a given hour in a particular month. For example, the hourly average heat loss at 1:00 am in January 2004 will be the average of the heat loss values calculated using equation 1 for 1:00 am each day from January 1st to January 31st, 2004. Similarly, the monthly total heat loss is the sum of the hourly heat loss for each hour and each day. The historical hourly average heat losses in Wh/m^2 and monthly total heat losses in kWh/m^2 are calculated for both insulated and uninsulated buildings. The historical heat loss values for a building, calculated using equations 2 and 3, represent the characteristics of heat loss for that building, which can be learned by ANN to predict future heat losses. Although heat loss is dependent on external temperature and wind speed according to equation 1, predicting heat loss over temperature and wind speed simplifies and speeds up the prediction process by reducing the number of parameters to be forecasted and the uncertainty related to the prediction of temperature and wind speed.

3.3. ANN prediction

The literature review indicates the successful use of feed-forward neural networks and different recurrent neural networks, such as NARnet, NARxnet, and LSTM neural networks, for predicting energy demand in buildings. Therefore, these four neural networks are considered for ANN analysis using the hourly average and monthly total heat loss data. The historical heat loss data from 2004 to 2019 are divided into training and test datasets, with different combinations ranging from 2 to 15 years. For example, if the training dataset includes data from 2004 and 2005, the test dataset will contain data from 2006 to 2019. Fourteen different combinations of training and test datasets are evaluated using the above-mentioned neural networks for both hourly and monthly heat loss prediction. In each case, the neural networks are used to predict the heat loss for the same length of data in the test dataset and compared against the test data to evaluate the performance of the neural network. In the training process of the hourly average heat loss prediction using a feed-forward neural network, the hour, month, and year are the three parameters considered as inputs, and the hourly average heat loss obtained from equation 2 is the output. In the case of monthly heat loss prediction using a feed-forward neural network, the month and year are the two input parameters, and the monthly heat loss obtained from equation 3 is the output for the network.

The recurrent neural network works differently than the feed-forward neural network, where the output of the previous time step is considered an additional input for the next time step. The training process of the recurrent neural network involves sequential training, and the time step is one of the default inputs for these networks. In the case of hourly average heat loss prediction, the hourly average heat loss obtained from equation 2 for the previous time step is chosen as the other input. For monthly heat loss prediction, the monthly total heat loss obtained from equation 3 is chosen as the second input instead of the hourly average heat loss. However, the NARxnet accepts additional inputs. Therefore, hour, month, and years are chosen as the additional inputs in the case of hourly average heat loss prediction, and month and year are chosen as the additional inputs in the case of monthly total heat loss analysis for NARxnet. The heat loss at the current time step is chosen as the output for all recurrent neural networks. For hourly average heat loss prediction, it will be the heat loss value obtained from equation 2, and for monthly total heat loss prediction, it will be the heat loss value obtained from equation 3.

4. RESULT AND DISCUSSION

To determine the best architecture for the artificial neural network (ANN), a sensitivity analysis is performed based on the number of layers and neurons in each layer. The training data set consists of the first four years of the entire data set (2004-2007), while the next four years (2008-2011) are used as the test data set. Heat loss data for insulated and uninsulated walls are included, and the average percentage error (APE) is used to measure performance. The feed-forward neural network can have multiple hidden layers with multiple neurons in each layer, so both the number of hidden layers and the number of neurons in each hidden layer are evaluated. Recurrent neural networks typically have one hidden layer with multiple neurons, so only one hidden layer is used for the NARnet, NARxnet, and LSTM networks in this study. The sensitivity analysis includes the number of neurons in the hidden layer for hourly average and monthly total heat loss predictions. Finally, the optimal ANN is used to predict heat loss for both insulated and uninsulated walls, and the energy savings are calculated based on the difference between the predicted heat loss for the two types of walls.

4.1. Sensitivity analysis

The sensitivity analysis for hourly average and monthly total heat loss predictions is presented in Figures 5 and 6, respectively. Figure 5-a shows the sensitivity of the number of hidden layers, while Figure 5-b shows the sensitivity of the number of neurons in each hidden layer for the feed-forward neural network. The sensitivity of the number of neurons in the hidden layer for recurrent neural networks is presented in Figure 5-c. From Figure 5-a, it is found that the average percentage error decreases as the number of hidden layers increases from two to six and then slightly increases with seven hidden layers. Figure 5-b shows that the minimum average percentage error is obtained with three neurons in each hidden layer. Therefore, the best network architecture for hourly heat loss analysis with the feed-forward neural network is composed of six hidden layers and three neurons in each hidden layer. From Figure 5-c, it is found that the NARnet and NARxnet networks show the lowest APE with 20 neurons in the hidden layer, while for the LSTM network, the minimum average percentage error is found with 40 and 140 LSTM cells in the hidden layer. However, the performances of all three recurrent neural networks are poor compared to the performance of the feed-forward network, possibly due to the small sample size of the training data set. Therefore, NARnet and NARxnet with 20 neurons in the hidden layer are selected for hourly heat loss prediction, while the LSTM network with 100 cells in the hidden layer is selected for hourly heat loss analysis due to previous research showing that 100 cells in the hidden layer provide the best performance without significantly increasing computing time.

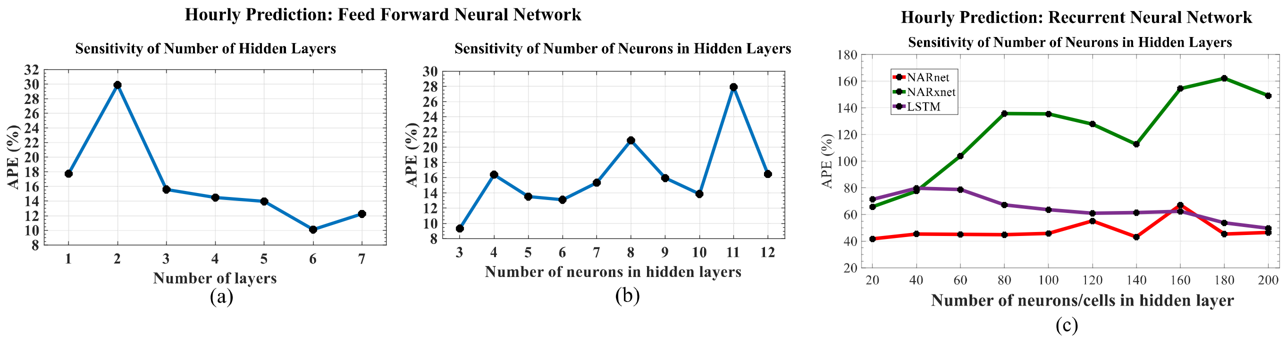

Figure 5 Results of sensitivity analysis for hourly heat loss

Figure 6 presents the sensitivity analysis for monthly predictions. From Figure 6-a and 6-b, it is found that the APE decreases with the increase in the number of hidden layers and increases with the increase in the number of neurons in a hidden layer. However, the APE reaches the minimum and remains stable between 10 to 12 hidden layers. Therefore, 11 hidden layers are selected as it is in the mid of the stable range. For the sensitivity of the number of neurons in a hidden layer, the minimum APE is obtained with two neurons in each hidden layer. Thus, the feed-forward network configuration with 11 hidden layers and two neurons in each hidden layer is selected for monthly heat loss prediction. Figure 6-c shows the sensitivity analysis results for NARnet and NARxnet networks and the LSTM neural network regarding the number of neurons/cells in the hidden layer. Again, the APE of the LSTM neural network is much lower than the APE of NARnet and NARxnet, as found in the first case study. The minimum APE for NARnet and NARxnet is found to be 60% with 12 neurons in the hidden layer, indicating poor prediction accuracy. However, these two networks are further considered to evaluate their performance with the full data set for monthly heat loss prediction. The APE of the LSTM neural network remains stable and below 10% with all different combinations of LSTM cells in the hidden layer. Therefore, the LSTM neural network with 12 cells in the hidden layer is selected for the current case study, as the same configuration showed excellent prediction accuracy in the first case study. Moreover, keeping the number of cells in the hidden layer as low as possible facilitates faster calculation in a shorter time.

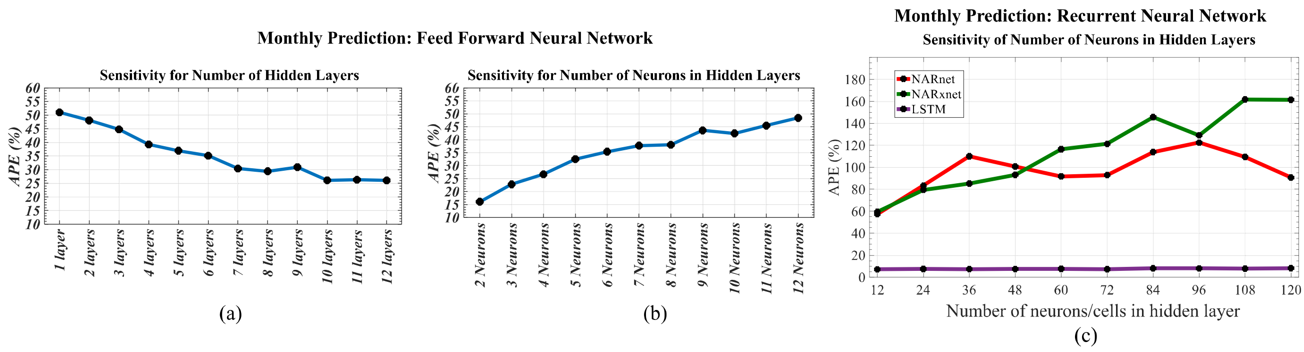

Figure 6 Results of sensitivity analysis for Monthly heat loss

4.2. Heat loss prediction

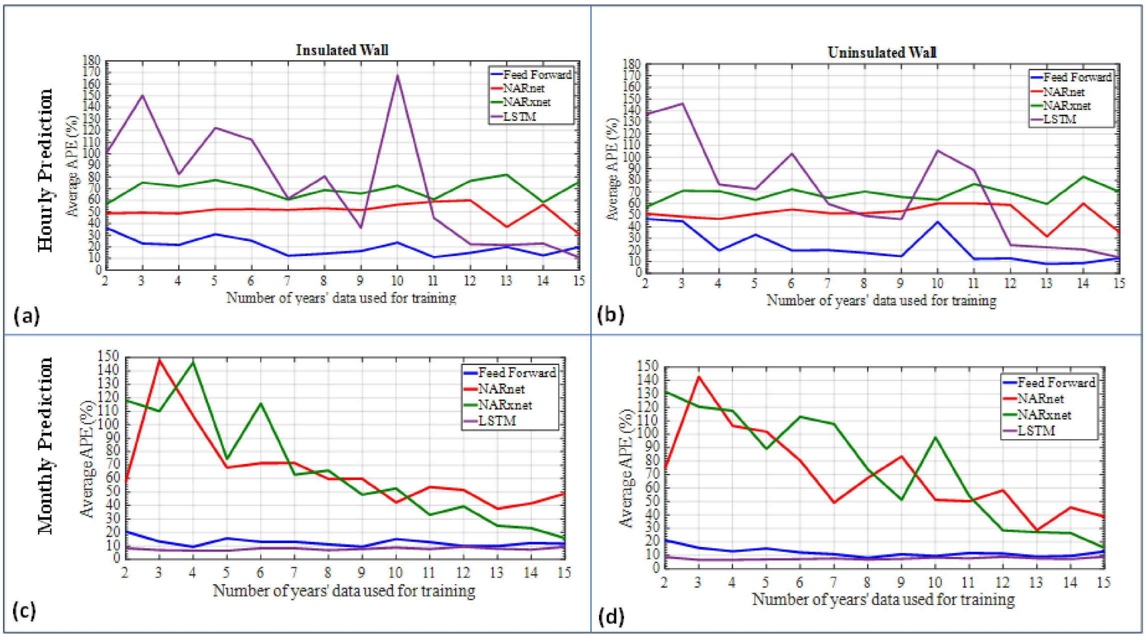

Figure 7 The comparison of performance among feed forward, NARnet, NARXnet and LSTM neural network

Figure 7 presents the average percentage errors (APE) in heat loss prediction for the feed-forward, NARnet, NARxnet, and LSTM neural networks trained using two to fifteen years of heat loss data. Among all four neural networks, the feed-forward neural network shows the lowest APE for the insulated wall in all cases, except when trained with 15 years of heat loss data (shown in Figure 7-a). The APE reaches around 10% when the feed-forward network is trained with 7 to 11 years of heat loss data. For the uninsulated wall, the APE of the feed-forward neural network is the lowest throughout all training cases (shown in Figure 7-b). The APE stays below 20% for both walls when the feed-forward network is trained with 7 years or more of heat loss data, except with 10 years of training. When the feed-forward network is trained with 10 years of heat loss data, the APE slightly goes over 20% for the insulated wall, while for the uninsulated wall, it jumps to around 40%. Despite this aberration in the uninsulated wall, the feed-forward network achieves 80% accuracy in all cases when trained with 7 years or more of heat loss data. The APE of NARnet and NARxnet mostly stays above 50%, except for NARnet, which shows below 40% APE when trained with 13 and 15 years of heat loss data, respectively. The LSTM neural network shows close to 20% APE when trained with 12 years or more of heat loss data, with the lowest APE achieved by the network trained with 15 years of heat loss data. Figures 7-c and 7-d show the mean percentage errors in monthly heat loss prediction for the insulated and uninsulated walls for different networks trained with 2 to 15 years of heat loss data. It is found from these two figures that the LSTM neural network shows the best performance in predicting monthly heat loss, with the APE remaining around 10% throughout. In comparing the feed forward neural network and the LSTM network, the APE of the former remains slightly higher, ranging between 10% and 20%. However, there are cases where the APE is the same for both networks, such as when the network is trained with 9 or 12 years of heat loss data for an insulated wall. Similar results are observed for an uninsulated wall when trained with 8 years and 10 years of heat loss data. The NARnet and NARxnet perform poorly compared to the LSTM and feed forward networks, with only NARxnet showing below 20% APE when trained with 15 years of heat loss data. The feed forward neural network is suitable for predicting hourly average heat loss with over 80% accuracy when trained between 7 and 9 years of heat loss data, while the LSTM network is 90% accurate for predicting monthly heat loss when trained with 8 years of data. Hence, for prediction of future heat loss for both hourly and monthly cases, the feed forward neural network is chosen for hourly heat loss prediction, and the LSTM network is chosen for monthly heat loss prediction. These predictions are made using 8 years of training data (2004 to 2007) to forecast the next 8 years (2012 to 2019) of heat loss. The predicted heat loss from these two ANNs is used in energy savings estimation. However, the NARnet and NARxnet are not recommended for hourly and monthly total heat loss prediction due to their high APE.

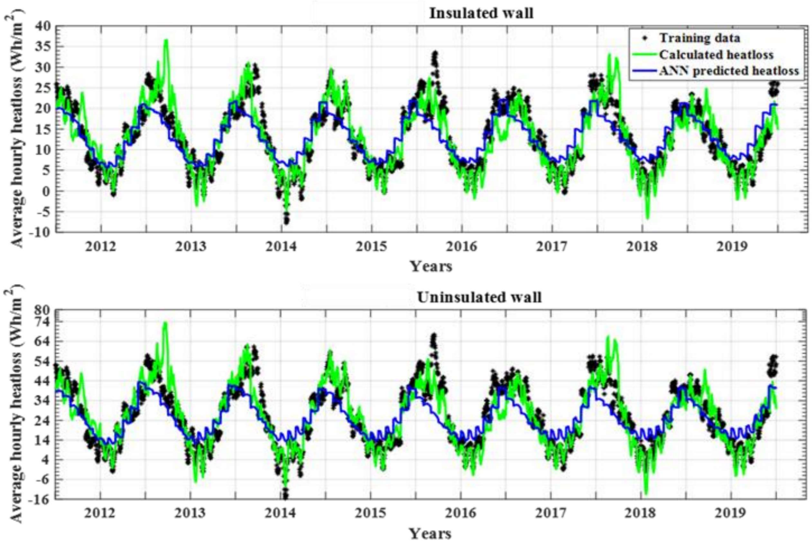

Figure 8 The comparison between the calculated and the ANN (feed forward) predicted hourly heat loss for the years 2012 to 2019

In Figure 8, the predicted heat loss curve of the feed forward neural network is compared to the calculated heat loss curve for both insulated and uninsulated walls from 2012-2019. Overall, the ANN predicted heat losses are very close to the calculated heat loss, with few exceptions. For example, the calculated heat loss is significantly higher in February and March of 2013 and 2018.

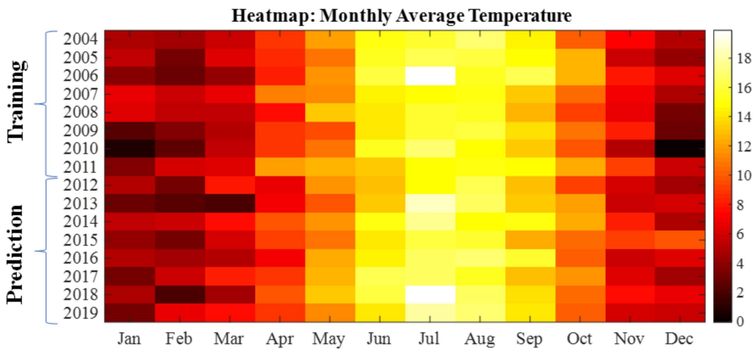

Figure 9 A heatmap representation of average temperature in each month from 2004 to 2019 in Nottingham

The heatmap of average temperature in Figure 9 shows that these months were cooler than in other years. Conversely, the calculated heat loss is far less than the ANN predicted heat loss for July 2013 and 2018, which were exceptionally warmer than in other years. The calculated heat loss curves also show negative heat loss or heat gain due to solar irradiation during the summer. This is not captured by the ANN prediction algorithm, which is designed to predict heat loss. However, this is sensible as heat gain during daytime summer does not contribute to heating energy savings, which is a key factor in estimating the payback period for retrofitting a building with improved insulation. In Figure 10, the calculated heat loss is compared to the LSTM neural network predicted heat loss for both insulated and uninsulated walls. It is observed that both the actual and ANN predicted heat loss curves have an identical trend, with some deviations noted. For example, the higher calculated heat loss in February-March of 2013 and 2018 can be attributed to extreme weather, as discussed in the hourly heat loss predictions.

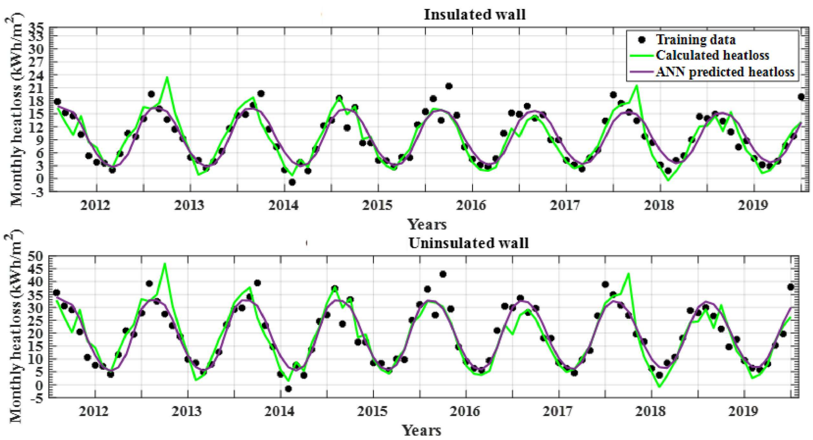

Figure 10 The comparison between the calculated and the ANN (LSTM) predicted monthly heat loss for the years 2012 to 2019

4.3. Energy savings

The case study presented in this paper demonstrates that the feed forward neural network is suitable for predicting hourly average heat loss, while the LSTM neural network is suitable for monthly total heat loss prediction with significant accuracy when trained with more than 8 years of heat loss data. However, it is also important to consider the estimated energy savings using ANN predicted heat losses. Figure 11 shows the estimated energy savings if an uninsulated building were retrofitted with improved insulation to match the level of an insulated building. The hourly average heat loss predicted by the feed forward network and the monthly total heat loss predicted by the LSTM neural networks are used for energy savings estimation, with all networks trained with 8 years of heat loss data. Energy savings are represented by the difference in yearly total heat loss between insulated and uninsulated buildings, calculated for the years 2012 to 2019. The calculated heat loss for both buildings in these years is compared to the ANN results. It is found that the difference between ANN predicted energy savings and calculated energy savings remains within ±15 kWh/m^2 (±10%) for all years except 2013, where the deviation is ±22 kWh/m^2 (±16%). Upon examining the heat map in Figure 9, it is observed that the winter in 2013 was cooler than any other year in the heat map, while the summer was warmer than any other year in the heat map. Therefore, extreme weather conditions in 2013 are responsible for the high deviation in ANN energy savings. The case studies confirm that the ANN can guarantee 84% accuracy in estimating energy savings, despite the influence of extreme weather conditions. It is highly unlikely to regularly experience extreme winters and summers like in 2013, and therefore, the ANN is expected to achieve 90% prediction accuracy in estimating energy savings in the majority of cases.

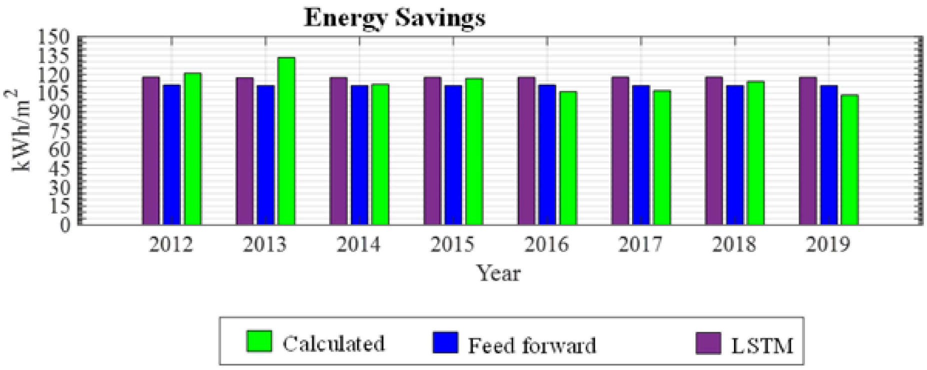

Figure 11 The comparison of energy savings for calculated heat loss and ANN predicted heat loss

5. CONCLUSION

Although monitoring of a building for years is a common practice for estimating energy savings, it is not always an accurate method due to the complex and variable nature of environmental parameters and human behaviour. However, this study presents a simplified novel approach that can provide sufficient information on future energy savings with reasonable accuracy by utilising AI and infrared thermography; combined with some reasonable assumptions. The use of AI in simple experimental work can allow for reasonable estimation of heat losses or energy savings, with ANN demonstrating an 84% accuracy rate in estimating energy savings according to the case studies. The LSTM neural network is suitable for monthly heat loss prediction, while the feed forward neural network is appropriate for hourly heat loss prediction. Both ANNs can accurately estimate heat loss with just 8 years of historic weather training data. The current study did not account for the impact of occupants' behaviour on energy savings. Future research will aim to include this factor to improve the estimation of energy savings.

6. REFERENCES

Al-Habaibeh, A., Medjdoub, B. and Pidduck, A., 2012. 'Investigating The Influence of Door Design on The Energy Consumption of Buildings Using Infrared Thermography', in *4th. JIIRCRAC 2012, Amman-Jordan, Sept. 10th – 12th 2012.*

Al-Habaibeh, A., Sen, A. And Chilton, J., 2021. Evaluation tool for the thermal performance of retrofitted buildings using an integrated approach of deep learning artificial neural networks and infrared thermography. Energy and Built Environment. ISSN 2666-1233.

Al-Habaibeh, A., Hawas, A., Hamadeh, L., Medjdoub, B., Marsh, J. and Sen, A., 2022. 'Enhancing the sustainability and energy conservation in heritage buildings: The case of Nottingham Playhouse', *Frontiers of Architectural Research*, 11(1), pp. 142–160. doi:10.1016/j.foar.2021.09.001.

AL-HABAIBEH, A., WATKINS, M., WARIED, K. and BATHAEI JAVARESHK, M., 2021. Challenges and opportunities of remotely working from home during Covid-19 pandemic. Global Transitions Proceedings. ISSN 2666-285X

Albatici, R. and Tonelli, A.M., 2010. 'Infrared thermovision technique for the assessment of thermal transmittance value of opaque building elements on site', *Energy and Buildings*, 42(11), pp. 2177–2183. doi:10.1016/j.enbuild.2010.07.010.

Albatici, R., Tonelli, A.M. and Chiogna, M., 2015. 'A comprehensive experimental approach for the validation of quantitative infrared thermography in the evaluation of building thermal transmittance', *Applied Energy*, 141, pp. 218–228. doi:10.1016/j.apenergy.2014.12.035.

Bienvenido-Huertas, D. *et al.,* 2019. 'Influence of ICHTC correlations on the thermal characterization of façades using the quantitative internal infrared thermography method', *Building and Environment*, 149, pp. 512–525. doi:10.1016/j.buildenv.2018.12.056.

BP PLC, 2021. *bp Statistical Review of World Energy*. Available at: https://www.bp.com/content/dam/bp/business-sites/en/global/corporate/pdfs/energy-economics/statistical-review/bp-stats-review-2022-full-report.pdf (Accessed: 10 August 2023).

Deb, C. *et al.,* 2017. 'A review on time series forecasting techniques for building energy consumption', *Renewable and Sustainable Energy Reviews*, 74, pp. 902–924. doi:10.1016/J.RSER.2017.02.085.

Department for Business Energy & Industrial Strategy, 2023. *ENERGY CONSUMPTION IN THE UK*. London. Available at: https://www.gov.uk/government/collections/energy-consumption-in-the-uk).

Gori, M., 2018. 'Deep Architectures', in *Machine Learning*. Elsevier, pp. 236–338. doi:10.1016/B978-0-08-100659-7.00005-1.

Government Property Agency, 2022. *NET ZERO PROGRAMME: Looking beyond carbon emissions*. Available at: https://www.gov.uk/government/case-studies/net-zero-programme-looking-beyond-carbon-emissions (Accessed: 10 August 2023).

Guan, Y. *et al.,* 2023. 'Burden of the global energy price crisis on households', *Nature Energy*, 8(3), pp. 304–316. doi:10.1038/s41560-023-01209-8.

Hochreiter, S. and Schmidhuber, J., 1997. 'Long Short-Term Memory', *Neural Computation*, 9(8), pp. 1735–1780. doi:10.1162/neco.1997.9.8.1735.

Kim, J. and Moon, J.W., 2009. 'Impact of Insulation on Building Energy Consumption', *Building Simulation 2009*, pp. 674–680. Available at: http://citeseerx.ist.psu.edu/viewdoc/summary?doi=10.1.1.172.4791.

Kolaitis, D.I. *et al.,* 2013. 'Comparative assessment of internal and external thermal insulation systems for energy efficient retrofitting of residential buildings', *Energy and Buildings*, 64, pp. 123–131. doi:10.1016/j.enbuild.2013.04.004.

Kossecka, E. and Kosny, J., 2002. 'Influence of insulation configuration on heating and cooling loads in a continuously used building', *Energy and Buildings*, 34(4), pp. 321–331. doi:10.1016/S0378-7788(01)00121-9.

Marino, B.M., Muñoz, N. and Thomas, L.P., 2017. 'Estimation of the surface thermal resistances and heat loss by conduction using thermography', *Applied Thermal Engineering*, 114, pp. 1213–1221. doi:10.1016/j.applthermaleng.2016.12.033.

Martellotta, F. *et al.,* 2017. 'On the use of artificial neural networks to model household energy consumptions', *Energy Procedia*, 126, pp. 250–257. doi:10.1016/j.egypro.2017.08.149.

Naji, S. *et al.,* 2016. 'Application of adaptive neuro-fuzzy methodology for estimating building energy consumption', *Renewable and Sustainable Energy Reviews*, 53, pp. 1520–1528. doi:10.1016/J.RSER.2015.09.062.

Nardi, I., Sfarra, S. and Ambrosini, D., 2014. 'Quantitative thermography for the estimation of the U-value: state of the art and a case study', *Journal of Physics: Conference Series*, 547, pp. 1–8. doi:10.1088/1742-6596/547/1/012016.

O'Grady, M., Lechowska, A.A. and Harte, A.M., 2017. 'Infrared thermography technique as an in-situ method of assessing heat loss through thermal bridging', *Energy and Buildings*, 135, pp. 20–32. doi:10.1016/j.enbuild.2016.11.039.

Papadopoulos, A.M., 2005. 'State of the art in thermal insulation materials and aims for future developments', *Energy and Buildings*, 37(1), pp. 77–86. doi:10.1016/j.enbuild.2004.05.006.

Piddington, J. *et al.,* 2020. *The Housing Stock of The United Kingdom*. Available at: https://files.bregroup.com/bretrust/The-Housing-Stock-of-the-United-Kingdom_Report_BRE-Trust.pdf (Accessed: 6 October 2020).

Reilly, A. and Kinnane, O., 2017. 'The impact of thermal mass on building energy consumption', *Applied Energy*, 198, pp. 108–121. doi:10.1016/j.apenergy.2017.04.024.

Ritchie, H., Roser, M. and Rosado, P., 2022. *Energy Production and Consumption*, *Published online at*

OurWorldInData.org. Available at: https://ourworldindata.org/energy-production-consumption (Accessed: 10 August 2023).

Sadineni, S.B., Madala, S. and Boehm, R.F., 2011. 'Passive building energy savings: A review of building envelope components', *Renewable and Sustainable Energy Reviews*, 15(8), pp. 3617–3631. doi:10.1016/j.rser.2011.07.014.

SALIM, S. and AL-HABAIBEH, A., 2023. Exploring windows opening behaviour of occupants of residential buildings using artificial intelligence. Energy and sustainable futures: proceedings of the 3rd ICESF, 2022. Cham: Springer, pp. 311-321. ISBN 9783031309595

Tabrizi, T.B., Hill, G. and Aitchison, M., 2017. 'The Impact of Different Insulation Options on the Life Cycle Energy Demands of a Hypothetical Residential Building', *Procedia Engineering*, 180, pp. 128–135. doi:10.1016/j.proeng.2017.04.172.

The National Energy Efficiency Network, 2019. *Energy consumption in new domestic buildings 2015 – 2017 (England and Wales)*. Available at: https://assets.publishing.service.gov.uk/government/uploads/system/uploads/attachment_data/file/853067/energy-consumption-new-domestic-buildings-2015-2017-england-wales.pdf (Accessed: 10 August 2023).

UN Environment Programme, 2020. *Building sector emissions hit record high, but low-carbon pandemic recovery can help transform sector – UN report*. Available at: https://www.unep.org/news-and-stories/press-release/building-sector-emissions-hit-record-high-low-carbon-pandemic (Accessed: 10 August 2023).

Wang, D. *et al.,* 2016. 'The influence of thermal insulation position in building exterior walls on indoor thermal comfort and energy consumption of residential buildings in Chongqing', *IOP Conference Series: Earth and Environmental Science*, 40, p. 012081. doi:10.1088/1755-1315/40/1/012081.

Wang, L., Lee, E.W.M. and Yuen, R.K.K., 2018. 'Novel dynamic forecasting model for building cooling loads combining an artificial neural network and an ensemble approach', *Applied Energy*, 228, pp. 1740–1753. doi:10.1016/j.apenergy.2018.07.085.

Wang, Z. and Srinivasan, R.S., 2017. 'A review of artificial intelligence based building energy use prediction: Contrasting the capabilities of single and ensemble prediction models', *Renewable and Sustainable Energy Reviews*, 75, pp. 796–808. doi:10.1016/J.RSER.2016.10.079.

Witten, I.H. *et al.,* 2017. 'Deep learning', in *Data Mining*. Elsevier, pp. 417–466. doi:10.1016/B978-0-12-804291-5.00010-6.

Xie, B. *et al.,* 2019. 'Evaluation of stearic acid/coconut shell charcoal composite phase change thermal energy storage materials for tankless solar water heater', *Energy and Built Environment* [Preprint]. doi:10.1016/j.enbenv.2019.08.003.